Journal of Power Sources 194 (2009) 976–980

Contents lists available at ScienceDirect

Journal of Power Sources

journal homepage: www.elsevier.com/locate/jpowsour

Short communication

Chromium nitride films on stainless steel as bipolar plate for proton exchange membrane fuel cell

Bo Wu [a], Yu Fu [b], Jun Xu [a], Guoqiang Lin [a,*], Ming Hou [c]

[a] Lab of Material Modification by Laser, Ion, and Electron Beams, Dalian University of Technology, Dalian, 116085, China
[b] Sunrise Power Co., Ltd., Dalian, 116025, China
[c] Fuel Cell R&D Center, Dalian Institute of Chemical Physics, Chinese Academy of Sciences, Dalian, 116023, China

ARTICLE INFO

Article history:
Received 9 June 2009
Accepted 9 June 2009
Available online 18 June 2009

Keywords:
Chromium nitride
Stainless steel bipolar plates
Pulsed bias arc ion plating

ABSTRACT

A series of chromium nitride films are prepared on stainless steel substrates by pulsed bias arc ion plating (PBAIP) at different N_2 flow rate as bipolar plates for proton exchange membrane fuel cell (PEMFC). The film chemical composition and phase structure are characterized by X-ray photoelectron spectroscopy (XPS) and X-ray diffractometry (XRD). The characterization results indicate that the nitrogen content of deposited films varies from 0.28 to 0.50, and the phase structure changes from mixtures of $Cr + Cr_2N$, pure Cr_2N through $Cr_2N + CrN$, to pure CrN. The interfacial contact resistance between samples and carbon paper is measured by Wang's method, and a minimum value of 5.8 $m\Omega\,cm^2$ is obtained under 1.2 MPa compaction force. The anticorrosion property is examined by potentiodynamic test in the simulated corrosive circumstance of the PEMFC under 25 °C, and the lowest corrosive current density of 5.9×10^{-7} A cm^{-2} is obtained at 0.6 V (vs. SCE). Stainless steel substrates coated by the film with lowest contact resistance are chosen as the bipolar plates to assemble cells. An average voltage value of 0.62 V is achieved at 500 mA cm^{-2}, which is close to that of the cell with Ag-plated bipolar plates.

1. Introduction

The proton exchange membrane fuel cell (PEMFC) is expected to be used in the many fields such as automotive application and portable power source due to its near-zero emission, fast start-up, high power density, high efficiency of energy conversion and low operation temperature [1]. As the most bulky, heavy and expensive section in the PEMFC [2,3], the bipolar plate plays an important role in supporting the cell stack, collecting current, separating the oxidants from fuels and channeling the oxidants and fuels. The ideal bipolar plate must have multifunctional characteristics such as good electrical conductivity, high corrosion resistance, high mechanical strength, low gas permeability, low cost and easy machining [4,5]. Except for the graphite bipolar plate, it is generally considered that only several noble metals such as gold and silver are optimal materials for manufacturing bipolar plate. But the high cost prevents them from the commercial realization. The stainless steels have the potential of being the candidate bipolar plate materials for their low electrical resistance, good thermal conductivity, excellent mechanical property and relatively low price [6]. But the corrosion resistance of stainless steels in fuel cell environment is not satisfied, and the Fe ions may dissolve more easily in an acidic environment which will result in the proton exchange membrane poison [7]. Surface modification by the high-quality, conductive and anticorrosive film is one of the solutions [8–14].

Chromium nitrides have good electrical conductivity and high corrosion resistance, so they are ideal surface coatings for stainless steel bipolar plate. Brady et al. [8–12] conducted a series of experiments on chromium nitrides. They formed chromium nitride films on different substrates including Ni50Cr alloy, 349™, AISI446, Ni–Cr based and Fe–Cr based commercial alloys, all samples showed improvement in corrosion resistance and electrical conductivity. In our previous work [13,14], pulsed bias arc ion plating (PBAIP) was employed to prepare chromium nitride films on stainless steel substrate. The potentiodynamic and potentiostatic characterization results showed that the corrosion resistance of the bipolar plate sample was greatly improved. The interfacial electrical conductivity of the sample was also improved.

In this paper, the composition and phase structure of chromium nitride films and the electric conductivity and corrosion resistance of the bipolar plates were investigated. The cell with the optimal chromium nitride film coated stainless steel plates was assembled and its initial performance was measured.

2. Experimental

The chromium nitride films were deposited on 316 L stainless steel plates in PBAIP system. Six kinds of chromium nitride films

* Corresponding author. Tel.: +86 411 84708380x8301.
E-mail address: gqlin@dlut.edu.cn (G. Lin).

0378-7753/$ – see front matter.
doi:10.1016/j.jpowsour.2009.06.029

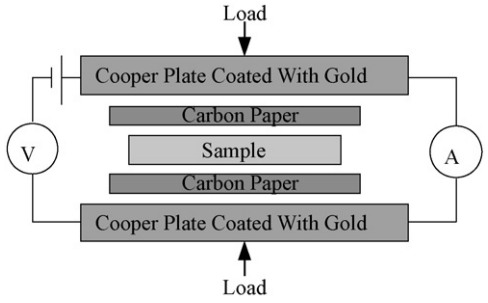

Fig. 1. Schematic illustration of interfacial contact resistance measurement equipment.

with various compositions were prepared by adjusting the N_2 flow rate. The pure metal chromium (99.9 wt.%) was used as the target. The chromium nitride films were deposited using a gas mixture of N_2 (99.99%) and Ar (99.99%), and the N_2 rates were kept at 20 sccm, 30 sccm, 40 sccm, 60 sccm, 70 sccm and 80 sccm and samples were numbered 1–6 respectively.

The chemical composition and chemical states of chromium nitride films were determined by the X-ray photoelectron spectroscopy (XPS) measurement with a VG ESCALAB MK2 spectrometer using a monochromated Al Kα (1486.6 eV) X-ray radiation. The phase structure of chromium nitride films was identified by X-ray diffractometry (XRD) using a 1.54 Å wavelength Cu Kα radiation with a D8-DISCOVER diffractometer.

The interfacial contact resistance between the sample and untreated Toray carbon paper was measured by Wang's method [15] using the setup as shown in Fig. 1. Two pieces of carbon paper were placed between the bipolar plate samples and two copper plates. The copper plates were coated with gold to enhance electrical conductivity. A compaction force was applied by using a WDW Electromechanical Universal Testing Machine with a step of 5 N s^{-1}. An electrical current of 5.0 A, sourced by a PSP-2010 Programmable power supply, was provided via the two plated copper plates during the tests.

Corrosion behaviors of the samples were investigated by potentiodynamic test in a 0.5 M H_2SO_4 + 5 ppm F^- solution, simulating the PEMFC environments. A conventional three-electrode system was used with a working electrode, a platinum sheet as the assistant electrode and a saturated calomel electrode (SCE, saturated KCl) as the reference electrode. The tests were conducted using a potentiostat Model 2273 A by EG&G Princeton Applied Research and analyzed with the corrosion software of EG&G Version 2.43.0. The dimensions of the working electrodes were 15 mm × 15 mm × 0.1 mm. The edges were protected by epoxy resin exposing 10 mm × 10 mm surface to the electrolyte. The tests were performed at 25 °C. Before every measurement, the sample was stabilized at open circuit potential for 30 min, then the potential was swept from −0.3 V to 0.8 V (vs. SCE) at a scanning rate of 2 mV s^{-1}.

Finally, the sample with the best performance in interfacial contact resistance measurement was chosen to assemble a cell for evaluating its initial performance. The parameters of the PEMFC stack are shown in Table 1.

Table 1
PEMFC stack operation conditions.

PEMFC stack parameters	Parameter values
Hydrogen pressure (inlet)/psi (gauge)	40
Oxygen pressure (inlet)/psi (gauge)	30
Cell temperature (°C)	55
Single cell potential range (V)	0.5–0.95
Humidification	Yes

Table 2
Chemical compositions of chromium nitride films evaluated from XPS data.

Sample no.	1	2	3	4	5	6
N_2 flow rate (sccm)	20	30	40	60	70	80
Nitrogen content (at.%)	0.28	0.36	0.41	0.50	0.50	0.50

3. Results and discussion

3.1. Composition of chromium nitride films

As is well known, XPS is a surface sensitive technique and therefore it is suitable to characterize the composition and the atoms chemical environments of a thin film. The chemical composition of the chromium nitride films evaluated from the XPS data is shown in Table 2. The results indicate that the nitrogen content increases from 0.28 to 0.50 as the N_2 flow rate increases from 20 sccm to 80 sccm. The chemical states of nitrogen and chromium atoms can be determined by the N1s and Cr2p spectra. The N1s and Cr2p XPS spectra for all samples of different N_2 flow rate as indicated with sample number on each spectrum, are shown in Fig. 2a and b respectively.

From Fig. 2a we could see, the N1s spectrum of sample 3, which is remarkably different from those of other samples, is composed of two separated peaks with binding energy centered at 396.6 eV and 397.5 eV, which could be contributed to Cr–*N* (396.6 eV) and Cr–*N*–Cr (397.5 eV) chemical states respectively [16]. The peaks of samples 1 and 2 are at 397.5 eV, corresponding a single chemical state of Cr–N–Cr, while those of samples 4, 5 and 6 are at 396.6 eV,

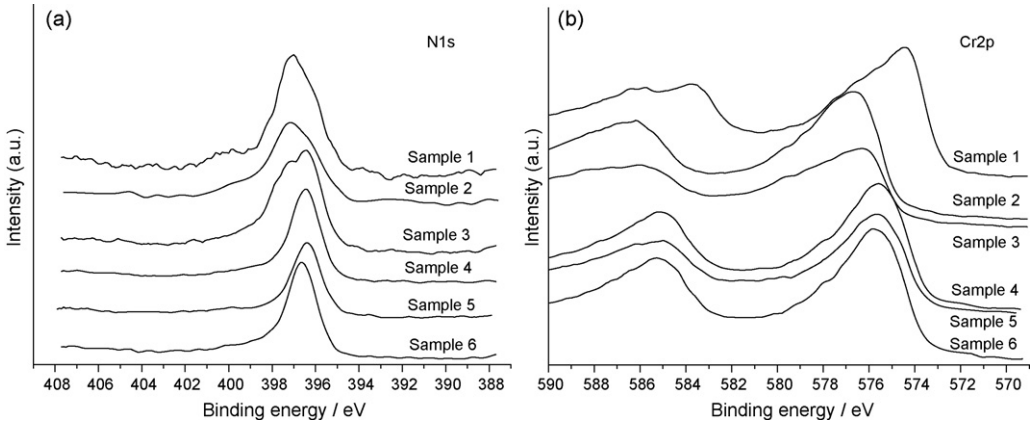

Fig. 2. N1s and Cr2p XPS spectra for all samples of different N_2 flow rate as indicated with sample number on each spectrum. (a) N1s spectrum and (b) Cr2p spectrum.

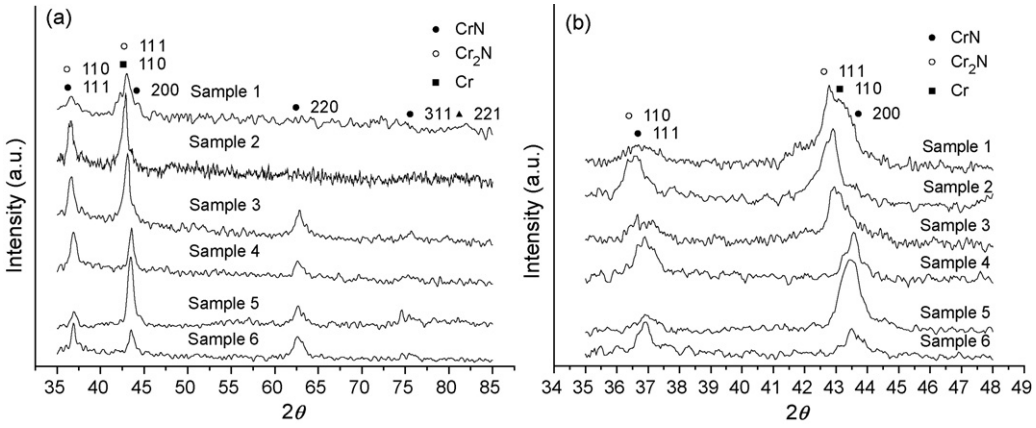

Fig. 3. X-ray diffraction spectra for all samples as a function of N_2 flow rate. (a) Full spectra and (b) enlarged spectra with diffraction angle of 2θ from 35° to 48°.

corresponding a single chemical state of N–Cr. In short, there are pure Cr–*N*–Cr type nitrogen atoms in samples 1 and 2, a mixture of Cr–*N*–Cr and Cr–*N* type nitrogen atoms in sample 3 and pure Cr–*N* type nitrogen atoms in samples 4, 5 and 6.

From the Cr2p XPS spectra in Fig. 2b three different Cr chemical states could be identified, i.e., *Cr*–*Cr* (metal Cr), *Cr*–N and *Cr*–N–*Cr* with binding energy centered at 574.0 eV, 575.8 eV, and 577.5 eV [16] respectively. There is a typical peak at low binding energy in the spectrum of sample 1 which corresponds to metal *Cr*. The peak of sample 2 is close to 577.5 eV, while those of samples 4, 5 and 6 are all centered at 575.8 eV. The peak of sample 3 appears at about 576.1 eV, between the electron binding energy of *Cr*–N–*Cr* and *Cr*–N. Based on the identification of the chemical state of nitrogen atoms, it is concluded from the analysis of the Cr2p spectra that there are a mixture of metal *Cr* and *Cr*–N–*Cr* type chromium atoms in sample 1, pure *Cr*–N–*Cr* type chromium atoms in sample 2, a mixture of *Cr*–N–*Cr* and *Cr*–N type nitrogen atoms in sample 3 and pure *Cr*–N type chromium atoms in samples 4, 5 and 6.

3.2. Phase structure of chromium nitride films

The XRD data for all samples indicate that different phases and orientation when the N_2 flow rate is changed. The full XRD spectra for all samples as a function of N_2 flow rate are shown in Fig. 3a, and the enlarged spectra with diffraction angle of 2θ from 35° to 48° are shown in Fig. 3b. For a N_2 flow rate of 20 sccm (sample 1), diffraction peaks corresponding to Cr_2N (1 1 0), Cr_2N (1 1 1), Cr_2N (2 1 1) and Cr (1 1 0) phases are detected. When the N_2 flow rate increases to 30 sccm (sample 2), the Cr (1 1 0) peak disappears and single hexagonal close-packed (HCP) Cr_2N phase with (1 1 0) and (1 1 1) peaks is identified. As the N_2 flow rate reaches 40 sccm (sample 3), besides the Cr_2N (1 1 0) and Cr_2N (1 1 1) peaks, a face-centered cubic (FCC) CrN phase with (1 1 1), CrN (2 2 0) and CrN (3 1 1) peaks is also observed in the spectra, indicating a two-phase mixture of Cr_2N and CrN is formed at a medium N_2 flow rate. Further increase the N_2 flow rates to 60 sccm, 70 sccm and 80 sccm (samples 4, 5 and 6), Cr_2N peaks disappears and the peaks corresponding to FCC CrN phase of (1 1 1), (2 0 0), (2 2 0) and (3 1 1) planes are all observed, indicating a single CrN phase structure is formed at higher N_2 flow rate, as clearly shown in Fig. 3b. Although samples 4, 5 and 6 are same in phase type, the CrN phase in sample 5 is observed with a remarkable (2 0 0) preferred orientation.

Combining the XPS results we could confirm that at lower N_2 flow rate of 20 sccm, the deposited film has a N-deficient Cr_2N phase structure with Cr clusters scattered in the film. At N_2 flow rate of 30 sccm, a single Cr_2N phase structure is formed, and at the medium N_2 flow rate of 40 sccm, more N atoms could be incorporated in the films and result in a two-phase mixture of Cr_2N and CrN. The nitrogen content in the film further increases with N_2 flow rate and a single phase CrN structure is realized at the N_2 flow rate higher than 60 sccm.

3.3. Interfacial contact resistance

The interfacial contact resistance between all samples coated with chromium nitride films and carbon paper was measured for different compaction force as shown in Fig. 4. The contact resistance deceases with the increase in compaction force. It is well known that this influence is due to the enlargement of the actual contact area between the sample and carbon paper. The interfacial contact resistance is in the range from 5.8 mΩ cm^2 to 24.5 mΩ cm^2 at a compaction force of 1.2 MPa. It can be seen from the curves that the performance of sample 5 ($Cr_{0.50}N_{0.50}$ film) is the best, and a minimum value of 5.8 mΩ cm^2 is obtained. The interfacial contact resistance of sample 2 ($Cr_{0.64}N_{0.36}$ film), which also reaches a quite low level of 6.4 mΩ cm^2 at 1.2 MPa compaction force, is slightly higher than that of sample 5 ($Cr_{0.50}N_{0.50}$ film). The results show the performance for all samples is in the order of sample 5 > sample 2 > sample 6 > sample 4 > sample 3 > sample 1. The above orders suggest that sample 5 is the best candidate to assemble the cell for testing the initial performance.

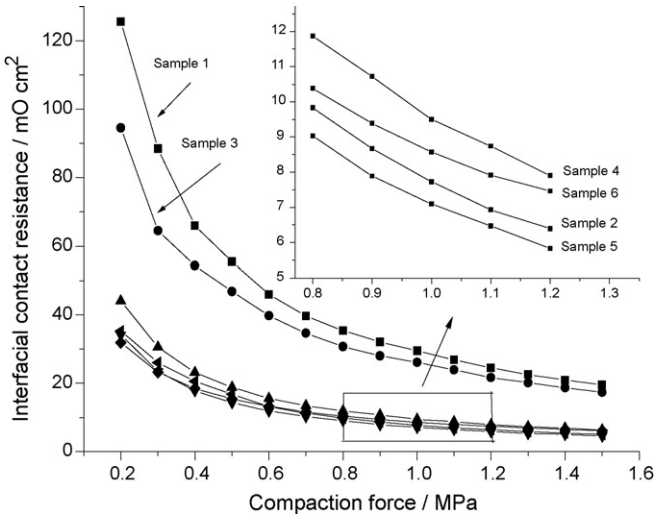

Fig. 4. Interfacial contact resistances between the samples and carbon paper under various compaction force.

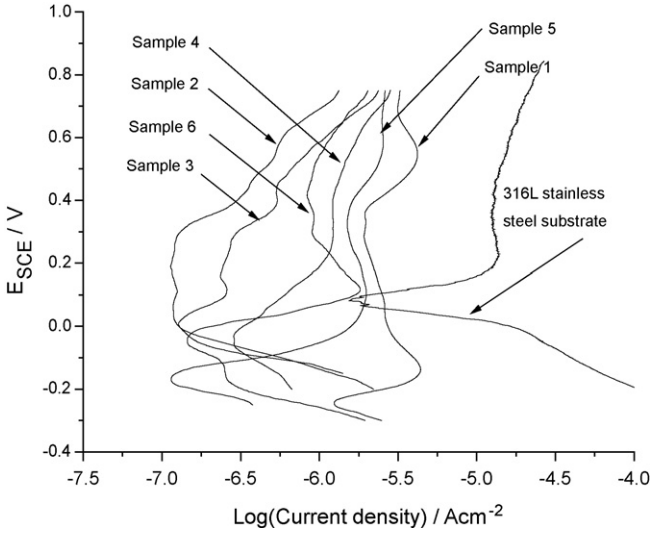

Fig. 5. Polarization behaviors of the stainless steel substrate and those coated with chromium nitride films examined by potentiodynamic test in a 0.5 M H_2SO_4 + 5 ppm F^- solution at 25 °C.

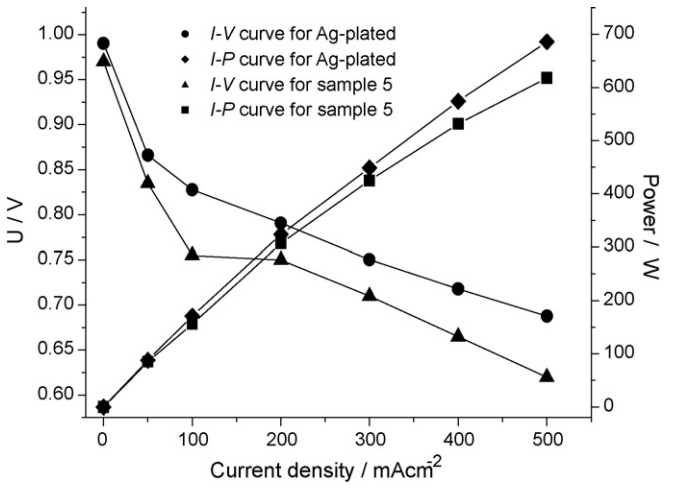

Fig. 6. *I–V* and *I–P* curves of the cell assembled with sample 5 and Ag-plated stainless steel bipolar plates.

The interfacial contact resistance is one of the key properties for bipolar plates and determines the power output of the cell. The investigation indicates that the interfacial contact resistance of stainless steel samples coated with chromium nitride films is greatly improved. The Cr_2O_3 layer, which is the main component of the passivation layer on the surface of stainless steel, being replaced by chromium nitride films contributes to the improvement in performance. The Cr_2O_3 compound belongs to ionic oxide, and the electric conductivity is poor for its ionic bonding. The chromium nitride is conductive ceramic material with the characteristics of both covalent compound and metal. So the chromium nitride generally exhibits much better electrical conductivity than that of chromium oxide such as Cr_2O_3. On the other hand, if the compaction force is large enough that the coated sample and carbon paper could be regarded to contact with each other "perfectly", the interfacial contact resistance will be almost determined by the inherent electrical conductivity of film material. In the case of the film consisting of multiple phases, the influence between different phases will result in the complicated aberration in crystal structure and enhance the electron wave scattering. The reduction of effective conductive electrons induces a decline in the inherent conductivity of film materials. So the contact conductivity of samples with either single CrN phase or single Cr_2N phase is higher than that of samples with multiple phases. In addition, although the samples 4, 5 and 6 are all composed of the same phase type, the CrN phase in sample 5 shows a remarkable (2 0 0) preferred orientation which indicates the arrangement of the CrN phase in sample 5 is more ordered than the other two samples. The more orderly arranged CrN phase will weaken electron wave scattering, so the electrical conductivity of sample 5 is a little better than that of samples 4 and 6.

3.4. Corrosion testing

Fig. 5 shows the polarization behaviors of the stainless steel substrate and those coated with chromium nitride films examined by potentiodynamic test in a 0.5 M H_2SO_4 + 5 ppm F^- solution at 25°C. The electrode potential is in the passive region for all samples at 0.6 V (vs. SCE), where the corrosive current density is in the range from 5.9×10^{-7} to 38.6×10^{-7} A cm^{-2}. All samples display much better anticorrosion property than bare 316L stainless steel. The sample 2 ($Cr_{0.64}N_{0.36}$ film) exhibits the best performance and achieve a minimum corrosive current density value of 5.9×10^{-7} A cm^{-2} which is one order of magnitude lower than that of stainless steel substrate (1.6×10^{-5} A cm^{-2} at 0.6 V). The characterization by potentiodynamic test indicates the samples' performance is in the order: sample 2 > sample 3 > sample 6 > sample 4 > sample 5 > sample 1.

The corrosion resistance is another key property for bipolar plates and influences the cell lifetime. The results indicate that the corrosion resistance of stainless steel bipolar plates coated with chromium nitride films is also greatly improved. The improvement in corrosion resistance has a close relation with the better chemical stability of the chromium nitride. The corrosion resistance of chromium nitride films is generally equal to that of the dense Cr_2O_3 passivation layer, but the native Cr_2O_3 layer formed in atmosphere has a loose structure, contains inclusions and contaminants. Comparing with the native Cr_2O_3 layer, the dense chromium nitride films prepared by PBAIP [17] in this experiment can more effectively protect the stainless steel substrate from corrosion in simulated circumstance. Additionally, the difference in the corrosion potential of different phases would result in forming micro-batteries which can greatly enhance the corrosion behavior. So the corrosion resistance of samples with a multiple phase structure is generally worse than that of the sample with a single phase structure.

4. Cell performances

Two single cells of stainless steel bipolar plates coated with the $Cr_{0.50}N_{0.50}$ film (sample 5) were assembled for initial performance test. Fig. 6 shows the *I–V* and *I–P* curves of the cell assembled with sample 5 and Ag-plated stainless steel bipolar plates respectively. Silver is a kind of noble metal with excellent electrical conductivity, so the stack with Ag-plated bipolar plates has good performance. It could be seen from the *I–V* and *I–P* curves that the performance of CrN-plated bipolar plates is almost the same as that of Ag-plated correspondence. When the current density is 500 mA cm^{-2}, the average voltages of Ag-plated and CrN-plated cells are 0.69 V and 0.62 V, and the average power is 686 W and 618 W respectively. The small difference in performance is mainly caused by the difference in contact resistance between the Ag-plated and CrN-plated bipolar plates.

5. Conclusions

The chromium nitride films were deposited on stainless steel bipolar plates for PEMFC by PBAIP. The experimental results show that nitrogen content of the films varies from 0.28 to 0.50, the

chromium nitride films consist of multiple phases of Cr and Cr_2N at low N_2 flow rate, a single phase of Cr_2N and multiple phases of Cr_2N and CrN as the N_2 flow rate increases, finally a single phase of CrN at high N_2 flow rate.

The performance of all samples in interfacial contact resistance and anticorrosion property test is improved. The sample 5 ($Cr_{0.50}N_{0.50}$ film) exhibits the lowest contact resistance and sample 2 ($Cr_{0.64}N_{0.36}$ film) shows the best corrosion resistance. The native Cr_2O_3 layer on stainless steel being replaced with the conductive and stable chromium nitride film is the main reason for the improvement in performance. Stack assembled with sample 5 shows good initial performance, which is close to that of the cell assembled with the Ag-plated bipolar plates. The results indicate chromium nitride film modified bipolar plates, especially the sample 5 ($Cr_{0.50}N_{0.50}$ film), have a great potential in application.

Acknowledgement

This work was financially supported by the National High Technology Research and Development Program of China (863 Program, No. 2007AA03Z221).

References

[1] K.B. Prater, J. Power Sources 51 (1994) 129–144.
[2] H. Tsuchiya, O. Kobayashi, Int. J. Hydrogen Energy 29 (2004) 985–990.
[3] K.S. Jeong, B.S. Oh, W. Kaiser, G. Böhm, J. Power Sources 105 (1) (2002) 58–65.
[4] H. Tawfik, Y. Hung, D. Mahajan, J. Power Sources 163 (2007) 755–767.
[5] V. Metha, J.S. Cooper, J. Power Sources 114 (2003) 32–53.
[6] J. Wind, R. Späh, W. Kaiser, G. Böhm, J. Power Sources 105 (2002) 256–260.
[7] M.J. Kelly, G. Fafilek, J.O. Besenhard, H. Kronberger, G.E. Nauer, J. Power Sources 145 (2005) 249–252.
[8] M.P. Brady, K. Weisbrod, I. Paulauskas, R.A. Buchanan, K.L. More, H. Wang, M. Wilson, F. Garzon, L.R. Walker, Scr. Mater. 50 (2004) 1017–1022.
[9] I.E. Paulauskas, M.P. Brady, H.M. Meyer III, R.A. Buchanan, L.R. Walker, Corros. Sci. 48 (2006) 3157–3171.
[10] H. Wang, M.P. Brady, G. Teeter, J.A. Turner, J. Power Sources 138 (2004) 86–93.
[11] H. Wang, M.P. Brady, K.L. More, H.M. Meyer III, J.A. Turner, J. Power Sources 138 (2004) 79–85.
[12] M.P. Brady, H. Wang, B. Yang, J.A. Turner, M. Bordignon, R. Molins, M. Abd Elhamid, L. Lipp, L.R. Walker, Int. J. Hydrogen Energy 32 (2007) 3778–3788.
[13] Y. Fu, M. Hou, G. Lin, J. Hou, Z. Shao, B. Yi, J. Power Sources 176 (2008) 282–286.
[14] Y. Fu, G. Lin, M. Hou, B. Wu, H. Li, L. Hao, Z. Shao, B. Yi, Int. J. Hydrogen Energy 34 (2009) 453–458.
[15] H. Wang, M.A. Sweikart, J.A. Turner, J. Power Sources 115 (2003) 243–251.
[16] S.M. Aouadi, D.M. Schultze, S.L. Rohde, K.-C. Wong, K.A.R. Mitchell, Surf. Coat. Technol. 140 (2001) 269–277.
[17] G. Lin, Y. Zhao, H. Guo, D. Wang, D. Chuang, R. Huang, L. Wen, J. Vac. Sci. Technol. A 22 (2004) 1218–1222.